

See discussions, stats, and author profiles for this publication at: <https://www.researchgate.net/publication/339773354>

Host expression system modulates recombinant Hsp70 activity through post-translational modifications

Article in *FEBS Journal* · March 2020

DOI: 10.1111/febs.15279

CITATION

1

READS

53

9 authors, including:



Maurício Menegatti Rigo

Universidade Federal do Rio Grande do Sul

39 PUBLICATIONS 225 CITATIONS

[SEE PROFILE](#)



Thiago J Borges

Brigham and Women's Hospital

44 PUBLICATIONS 633 CITATIONS

[SEE PROFILE](#)



Benjamin J Lang

Beth Israel Deaconess Medical Center

27 PUBLICATIONS 148 CITATIONS

[SEE PROFILE](#)



Ayesha Murshid

Beth Israel Deaconess Medical Center

52 PUBLICATIONS 1,572 CITATIONS

[SEE PROFILE](#)

Some of the authors of this publication are also working on these related projects:



Special Issue "Eukaryotic Transcription Initiation and Elongation Mechanisms" [View project](#)



Structural analysis of DnaK [View project](#)

Host expression system modulates recombinant Hsp70 activity through post-translational modifications

Mauricio M. Rigo¹ , Thiago J. Borges² , Benjamin J. Lang³ , Ayesha Murshid³ , Nitika⁴ , Donald Wolfgeher⁵ , Stuart K. Calderwood³ , Andrew W. Truman⁴  and Cristina Bonorino^{6,7} 

1 School of Medicine, Pontificia Universidade Catolica do Rio Grande do Sul, Porto Alegre, Brazil

2 Schuster Family Transplantation Research Center, Department of Medicine, Brigham and Women's Hospital, Harvard Medical School, Boston, MA, USA

3 Department of Radiation Oncology, Beth Israel Deaconess Medical Center, Harvard Medical School, Boston, MA, USA

4 Department of Biological Sciences, The University of North Carolina at Charlotte, Charlotte, NC, USA

5 Department of Molecular Genetics and Cell Biology, The University of Chicago, Chicago, IL, USA

6 Laboratório de Imunoterapia, Universidade Federal de Ciências da Saúde de Porto Alegre, Porto Alegre, Brazil

7 Department of Surgery, School of Medicine, University of California at San Diego, La Jolla, CA, USA

Keywords

heat shock protein; post-translational modifications; DnaK; *Escherichia coli*; *Pichia pastoris*

Correspondence

M. M. Rigo, School of Medicine, Pontificia Universidade Catolica do Rio Grande do Sul, Av. Ipiranga, 6681, Porto Alegre, Rio Grande do Sul, ZIP CODE 90619-900, Brazil.
Tel: +55519981804574
E-mail: mauriciomr1985@gmail.com

Mauricio M. Rigo and Thiago J. Borges are co-first authors

(Received 16 July 2019, revised 22 January 2020, accepted 23 February 2020)

doi:10.1111/febs.15279

The use of model organisms for recombinant protein production results in the addition of model-specific post-translational modifications (PTMs) that can affect the structure, charge, and function of the protein. The 70-kDa heat shock proteins (Hsp70) were originally described as intracellular chaperones, with ATPase and foldase activity. More recently, new extracellular activities of Hsp70 proteins (e.g., as immunomodulators) have been identified. While some studies indicate an inflammatory potential for extracellular Hsp70 proteins, others suggest an immunosuppressive activity. We hypothesized that the production of recombinant Hsp70 in different expression systems would result in the addition of different PTMs, perhaps explaining at least some of these opposing immunological outcomes. We produced and purified *Mycobacterium tuberculosis* DnaK from two different systems, *Escherichia coli* and *Pichia pastoris*, and analyzed by mass spectrometry of the protein preparations, investigating the impact of PTMs in an *in silico* and *in vitro* perspective. The comparisons of DnaK structures *in silico* highlighted that electrostatic and topographical differences exist that are dependent upon the expression system. Production of DnaK in the eukaryotic system dramatically affected its ATPase activity and significantly altered its ability to downregulate MHC II and CD86 expression on murine dendritic cells (DCs). Phosphatase treatment of DnaK indicated that some of these differences related specifically to phosphorylation. Altogether, our data indicate that PTMs are an important characteristic of the expression system, with differences that impact interactions of Hsps with their ligands and subsequent functional activities.

Abbreviations

ACN, acetonitrile; ADP, adenosine diphosphate; AP, alkaline phosphatase; ATP, adenosine triphosphate; BCA, bicinchoninic acid; CD, cluster of differentiation; CCR5, C-C chemokine receptor type 5; DCs, dendritic cells; *E. coli*, *Escherichia coli*; FBS, fetal bovine serum; FPLC, fast protein liquid chromatography; Gly, glycine; GTP, guanosine triphosphate; Hsp, Heat shock protein; HPLC, high-performance liquid chromatography; Hsp70, 70-kDa heat shock protein; IL-10, interleukin 10; LC-MS/MS, electrospray tandem mass spectrometry; LOX-1, lectin-type oxidized LDL receptor 1; *M. tuberculosis*, *Mycobacterium tuberculosis*; March1, membrane associated RING-CH 1; MHC II, major histocompatibility complex class II; MOPS, 3-(N-morpholino)propanesulfonic acid; NBD, nucleotide binding domain; *P. pastoris*, *Pichia pastoris*; PBS, phosphate-buffered saline; PTMs, post-translational modifications; SBD, substrate binding domain; SDS/PAGE, sodium dodecyl sulfate–polyacrylamide gel electrophoresis; TBS, Tris-buffered saline; TBST, Tris-buffered saline tween; TFA, trifluoroacetic acid.

Database

Mass spectrometry proteomic data are available in the PRIDE database under the accession number PXD011583.

Introduction

Heat shock protein 70s (Hsp70s) are a highly conserved class of molecular chaperones that fold a large proportion of the proteome [1-4]. Hsp70 is comprised of four major structural domains: a region that binds ATP called nucleotide binding domain (NBD); a region that binds client proteins (usually hydrophobic peptides) referred to as substrate binding domain (SBD); a linker segment of few residues that physically connects NBD and SBD; and a C-terminal region that functions as a 'lid', participating in Hsp70 substrate turnover. The Hsp70 mode of action favors the existence of two extreme conformations: an open state, in which the ATP is bound and the affinity for the substrate is low; and a closed state, in which ATP hydrolysis favors substrate binding to the SBD [5,6].

Hsp70 has been extensively studied; however, little is known about the post-translation modifications (PTMs) of Hsp70 and how they might affect its function. Global proteomic studies have uncovered a wide range of PTMs on Hsp70 isoforms in different organisms that include phosphorylation, acetylation, and ubiquitylation. Recent evidence suggests that even single PTMs on Hsp70 can dramatically alter ATPase activity, folding of clients, and localization in the cell [7-9]. It is becoming clear that these modifications form a 'chaperone code' that acts as a crossroads for cellular signaling and fine-tunes Hsp70 function [10,11].

Although heat shock proteins (Hsps) were described originally as intracellular proteins (e.g., cytosol, nucleus, endoplasmic reticulum) [12-14], they were later found to be also present in the extracellular milieu [15,16], secreted by a nonclassical route [17,18]. The extracellular roles of Hsps are not completely understood. For example, studies investigating the inflammatory properties of extracellular Hsps have on occasion reported opposing activities of Hsp70 proteins that have led to some ambiguity in the field. While some describe an immunostimulatory role for extracellular mammalian Hsp70 [19], results by other groups demonstrate this observation is at least in part explainable by bacterial contaminants [20,21]. However, while most studies of the potential immunomodulatory roles of Hsp70 carried out *in vivo* indicate a pro-inflammatory effect [22], studies utilizing DnaK

(bacterial Hsp70) purified from *Mycobacterium tuberculosis* (*M. tuberculosis*) demonstrated an anti-inflammatory effect [23].

Studies on extracellular functions of Hsp70s commonly utilize proteins obtained from different sources. Model organisms used for recombinant protein production such as *Escherichia coli* and *Pichia pastoris* (*P. pastoris*) have unique advantages that include ease of use, cellular doubling time, cost, and scalability [24]. Importantly, although some *E. coli* proteins were already identified with the presence of serine, threonine, or tyrosine phosphorylation [25,26], this system generally does not carry out these PTMs, a benefit or disadvantage depending on the desired downstream application of the recombinant protein. It is possible that some of the contradictory results observed in the literature using recombinant Hsp70 could at least in part be explained by host-induced PTMs.

In this study, we hypothesized that the production of recombinant Hsp70 in different expression systems would result in the addition of different PTMs. To characterize differences in Hsp70 PTMs created by expression in different hosts, we used mass spectrometry to analyze protein preparations of DnaK from *M. tuberculosis* expressed in two different expression systems (*E. coli* and *P. pastoris*). DnaK from *M. tuberculosis* is largely used as an Hsp70 model due to structural homology with Hsp70 proteins from other organisms; also, the sequence similarity after a pairwise alignment with DnaK from *E. coli* is over 70% (UniProt ID P9WMJ9 and P0A6Y8 submitted to EMBOSS-NEEDLE server). We analyzed the impact of PTMs in an *in silico* perspective in a complete DnaK structure obtained from homology modeling. Functional analysis of each DnaK preparation was evaluated in ATPase activity assays, and also in immunomodulation assays, assessing their ability to reduce MHC II and CD86 expression in dendritic cells [27].

Our results revealed that several of the PTMs within the functional domains of DnaK differ between expression systems. The comparisons of *in silico* structures highlighted the electrostatic, topographical, and accessible surface area differences between the two expression systems. Production of DnaK (a bacterial protein) in a eukaryotic system dramatically affected

its ATPase activity, but not its ability to interact with DnaJ. It significantly altered its effects on the down-regulation of MHC II and CD86 expression on murine dendritic cells. At least part of these alterations could be explained by differences in phosphorylation, as evidenced by phosphatase treatment. Altogether, our data indicate that PTMs are an important characteristic of the expression system, and provide evidence to show how these can impact functional interactions of Hsps with their ligands.

Results

Identification of PTMs in recombinant M. tuberculosis DnaK expressed in *Escherichia coli* and *Pichia pastoris*

We used mass spectrometry to detect PTMs on DnaK expressed and purified from *E. coli* and *P. pastoris*. Acetylation and Gly-Gly were detected on DnaK purified from both *E. coli* and *P. pastoris*, while phosphorylation was only detected on DnaK expressed in the eukaryotic system (Fig. 1A). Interestingly, there was a substantial overlap on PTMs seen on DnaK purified from both systems; 52% of the total DnaK acetylation sites detected were identical in both systems, and 33% of Gly-Gly mods were conserved (Fig. 1B).

Assessment of PTMs by functional domains of DnaK after expression in *Escherichia coli* and *Pichia pastoris*

We also evaluated each set of PTMs according to the functional domains NBD, SBD, linker, and Lid in a structural perspective using *in silico* models of DnaK (Fig. 1C). We inserted all identified PTMs in an *in silico* model using PyTMs, a PyMOL plug-in. Due to limitations of the plug-in, and because we cannot precisely identify the type of Gly-Gly modification, we focused our analysis on acetylation and phosphorylation, which are among the most frequent PTMs reported experimentally and nonexperimentally in the Swiss-Prot Knowledgebase [28].

Regarding the NBD domain (Fig. 2A), the modified residues significantly changed the protein's molecular surface both electrostatically and topographically. The identified acetylated and phosphorylated sites favored a more negative landscape, compared to the model without any PTMs. An overall negative charge on the NBD is especially favored when the protein is purified from *P. pastoris*. We noted that acetylated residues K55, K240, and K242 are close to the ATP binding site of the NBD (Fig. 2B). Of these, only K242 was

conserved between *E. coli* and *P. pastoris*, while K55 and K240 were found only in *P. pastoris*.

Regarding the comparison of SBD domains, we could not find acetylation or phosphorylation after expression in the *E. coli* system (Fig. 3A). In *E. coli*, the only PTM observed was a Gly-Gly modification on Lysine 463. In *P. pastoris*, however, acetylation, phosphorylation, and Gly-Gly modifications were present. Overall, the *P. pastoris* PTMs also added a more negative aspect to the SBD (Fig. 3A). This could influence the binding of client proteins. In one specific case, residue K378, which is acetylated only in *P. pastoris*, is close to the client binding site (Fig. 3B).

The Lid domain of DnaK expressed in *P. pastoris* also presented more PTMs with respect to *E. coli* (Fig. 4). These modifications could have an impact on the open-closed dynamics of DnaK, in its interactions with other proteins, or even in the oligomerization of DnaK, as discussed below.

We have not observed PTMs directly added to residues in the linker region (residues 362 to 367); however, a lysine at position 361, next to the linker, was found to be acetylated and with a Gly-Gly modification in both expression systems. Also, in the proximity, threonine 369 was phosphorylated, but only in *P. pastoris*.

Electrostatic potential analysis highlights differences between expression systems

We analyzed each PTM regarding its electrostatic potential, comparing the proteins with or without the PTMs found in both expression systems. In Fig. 5A and Movie S1, we summarize the impact of PTM in each protein according to the expression system. In general, we observed that DnaK expressed in *P. pastoris* presents a more negative landscape with respect to DnaK expressed in *E. coli* or even if DnaK was without any PTM.

DnaK activity changes depending on the expression system

To investigate whether DnaK produced in different expression systems would present different functional properties due to the differences in the PTM profile, we used two approaches. We first assayed an extensively described property of DnaK, its ability to bind and reduce ATP to ADP. For that, we used a colorimetric ATPase assay, testing different concentrations of DnaK (0–1.5 μM) for its ATP hydrolysis capacity. DnaK expressed in the *E. coli* system presented a significantly superior ATPase activity than the DnaK expressed in *P. pastoris* (Fig. 6A).

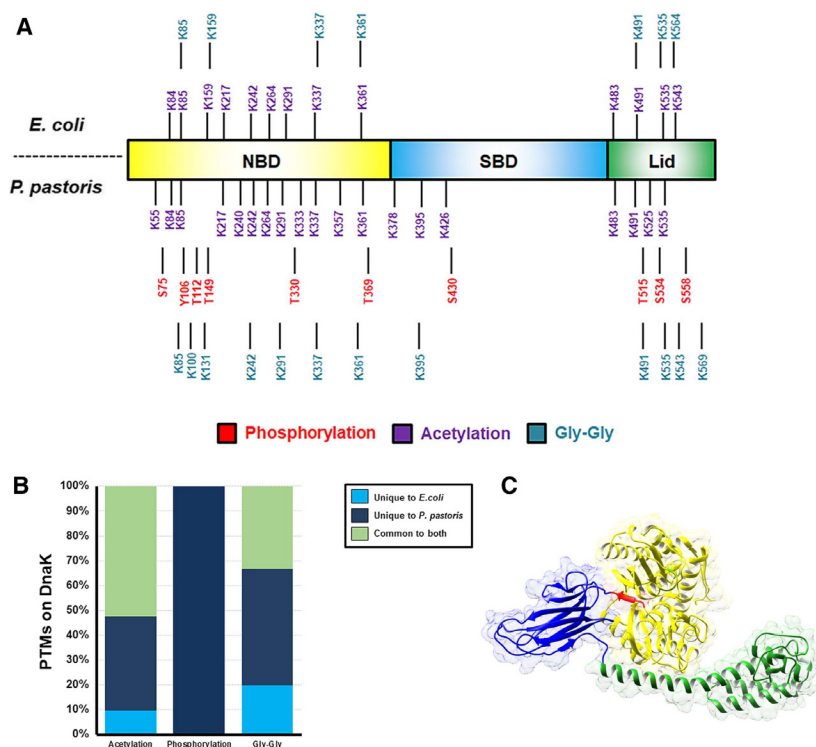


Fig. 1. Localization and occurrence of post-translational modifications (PTMs) found in DnaK after *E. coli* and *P. pastoris* expression. (A) Specific position of each PTM (phosphorylation in red, acetylation in purple, and Gly-Gly in blue) in each of the DnaK domains. *E. coli* and *P. pastoris* modifications are located above and below the graphical representation, respectively. (B) Mosaic plot used to represent the percentage of each PTM on DnaK that are unique to *E. coli*, unique to *P. pastoris* or common to both. (C) DnaK model created based on PDBs IDs 4B9Q and 4JN4. The C-terminal region was modeled by *ab initio* approach. The nucleotide binding domain (NBD) is shown in yellow; the substrate binding domain (SBD) is shown in blue and the Lid domain in green. The short red segment represents the linker region between the NBD and the SBD. The figure was built using the software UCSF Chimera.

To test whether the difference in ATPase activity could be due to phosphorylation, which was only present in DnaK purified from *P. pastoris*, we treated DnaK produced in that system with alkaline phosphatase (AP), which significantly removed the phosphoserine domains (Fig. 6B). AP treatment improved the ATP hydrolysis capacity of the DnaK expressed in *P. pastoris* to levels similar to the observed in DnaK expressed in *E. coli* (Fig. 6C). Notably, the incubation of DnaJ in combination with DnaK from both systems significantly improved ATPase activity (Fig. 6C), indicating that DnaK interaction with DnaJ was not negatively affected by phosphorylation. DnaJ had a greater effect in improving the ATPase activity of DnaK expressed in *P. pastoris* (a ~ 32-fold change) compared to DnaK expressed in *E. coli* (a ~ 1.8-fold change) (Fig. 6C, second column vs the fourth column).

Extracellular DnaK decreases the expression of two dendritic cells (DCs) activation markers—MHC II and CD86 [29]. We have recently elucidated the molecular pathway of this modulation, which is dependent on DnaK induction of March1 via IL-10 [30], leading to ubiquitination and degradation of those two molecules. To test the functional relevance of the different PTM profiles found, we treated mouse DCs isolated from mouse secondary lymphoid organs (spleen and lymph nodes) with *M. tuberculosis* DnaK made in

E. coli or *P. pastoris* and analyzed the expression of MHC II and CD86 by flow cytometry. As expected, DnaK produced in *E. coli* decreased both MHC II (Fig. 6D) and CD86 (Fig. 6E). However, the effect of DnaK produced in *P. pastoris* was significantly more pronounced than the one expressed in *E. coli* (Fig. 6D,E). Treatment of DnaK with alkaline phosphatase reversed the suppression of both MHC II and CD86 expression (Fig. 6D,E). Thus, the expression system used to prepare recombinant proteins is important for their functional properties both as an intracellular chaperone and extracellular signaling ligand, most probably due to the different PTM profiles found (DnaK in *E. coli* vs *P. pastoris*). Additionally, part of these alterations could be explained by differences in phosphorylation present only in the DnaK expressed in the *P. pastoris* system.

Discussion

Post-translational modifications are pivotal in determining how proteins interact with their ligands, their dynamics in the environment, and their functions. We demonstrated here that DnaK from *M. tuberculosis*, a bacterial Hsp70 homologous protein, acquires different PTMs depending on the expression system (*E. coli* or *P. pastoris*). These modifications alter the protein's ATPase function and also seem to play a role in the

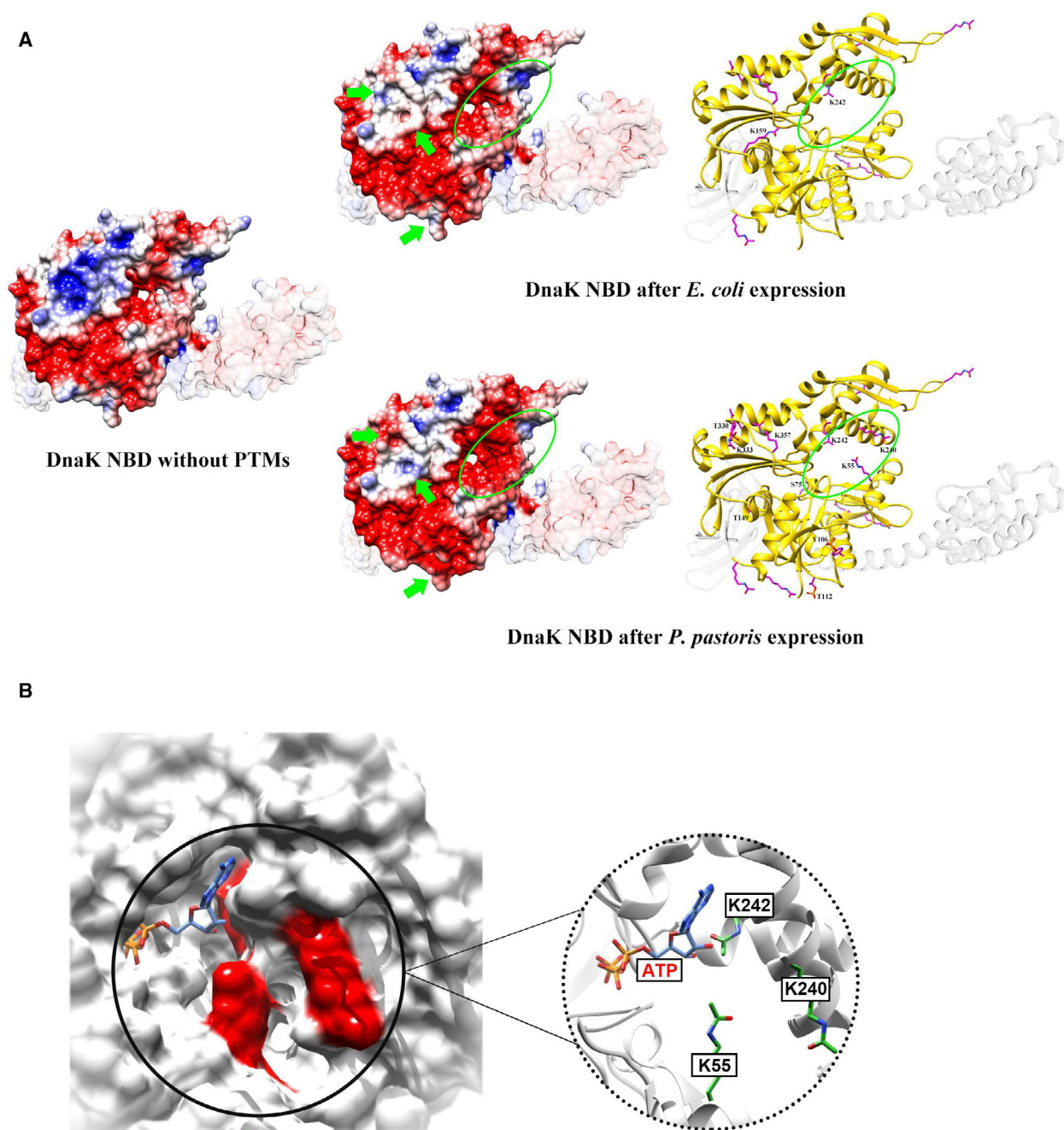


Fig. 2. Surface and ribbon representation of the DnaK model, with emphasis on the NBD. (A) The electrostatic potential was computed on the surface, and the color range indicates the positive (*blue*), neutral (*white*), and negative (*red*) charges ($-3 kT$ to $+3 kT$, where k represents the Boltzmann constant and T represents the temperature). The arrows and the ellipse highlight charges and topographical differences between proteins expressed in each system. The ellipse area corresponds to residues K55, K240, and K242. (B) NBD representation with emphasis in three modified residues: K55, K240, and K242. The figure in the left is a surface representation of the DnaK NBD (K55, K240, and K242 colored in red) and a sticks representation of ATP. The figure in the right highlights the proximity among the lysine residues and the ATP. The figures were build using the software UCSF Chimera.

immunomodulation promoted by DnaK on MHC II and CD86 expression of dendritic cells. Frequent modifications such as phosphorylation and acetylation

impact the general landscape of the protein, modifying electrostatic potential and protein topography, which could explain the different behavior of DnaK in

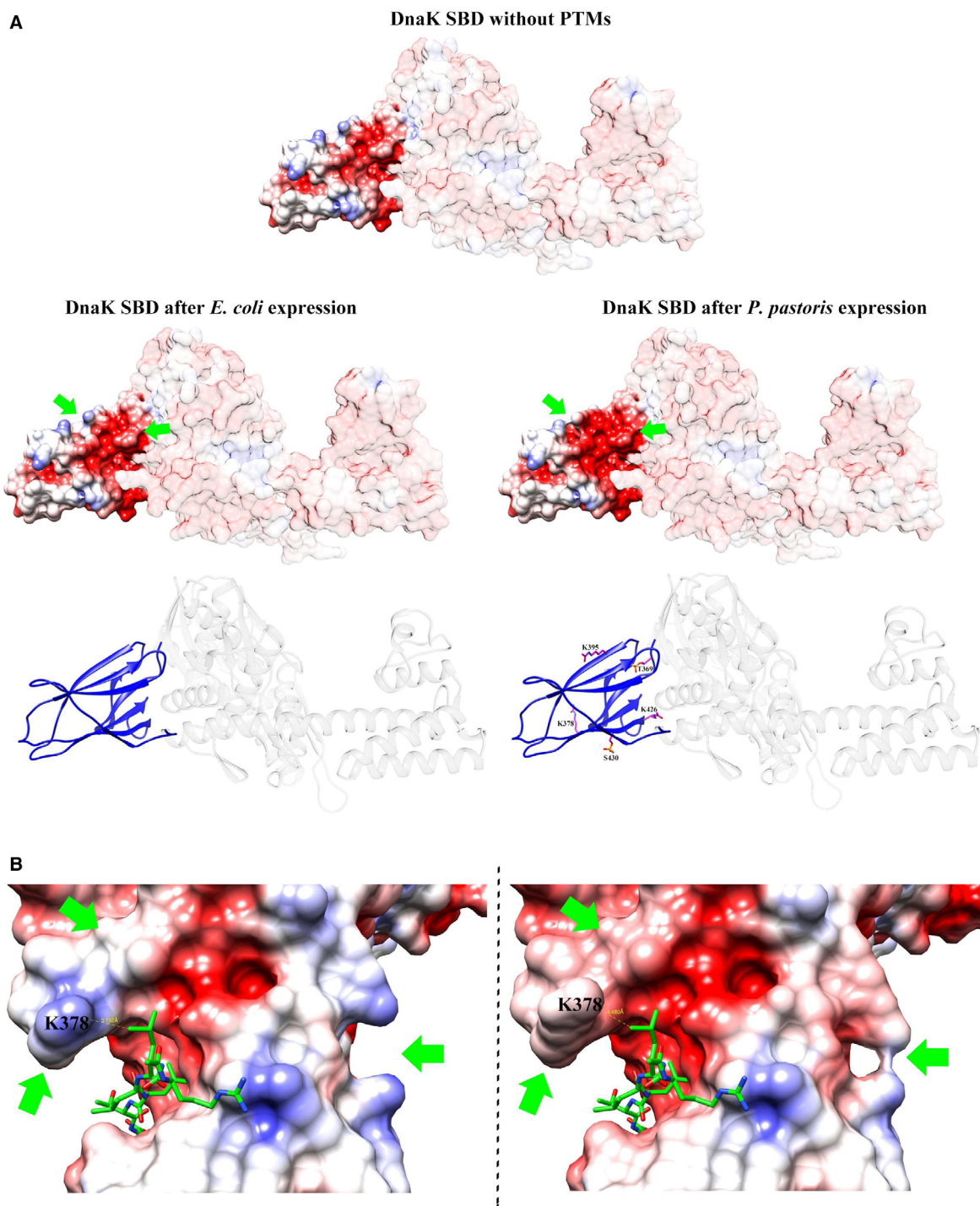


Fig. 3. Surface and ribbon representation of the DnaK model, with emphasis on the SBD. (A) The electrostatic potential was computed on the surface, and the color range ($-3 kT$ to $+3 kT$, where k represents the Boltzmann constant and T represents the temperature) indicates the positive (*blue*), neutral (*white*), and negative (*red*) charges. The arrows highlight the charges and topographical differences between proteins expressed in each system. (B) DnaK SBD comparison after expression in *E. coli* (left) and *P. pastoris* (right). A client protein represented by the sequence NRLLLTG (green) was added from PDB structure 4PO2 to give some perspective about the binding site and the distance to residue K378. Arrows indicate charges and topographical differences closed to client binding site. The figures were built using the software UCSF Chimera.

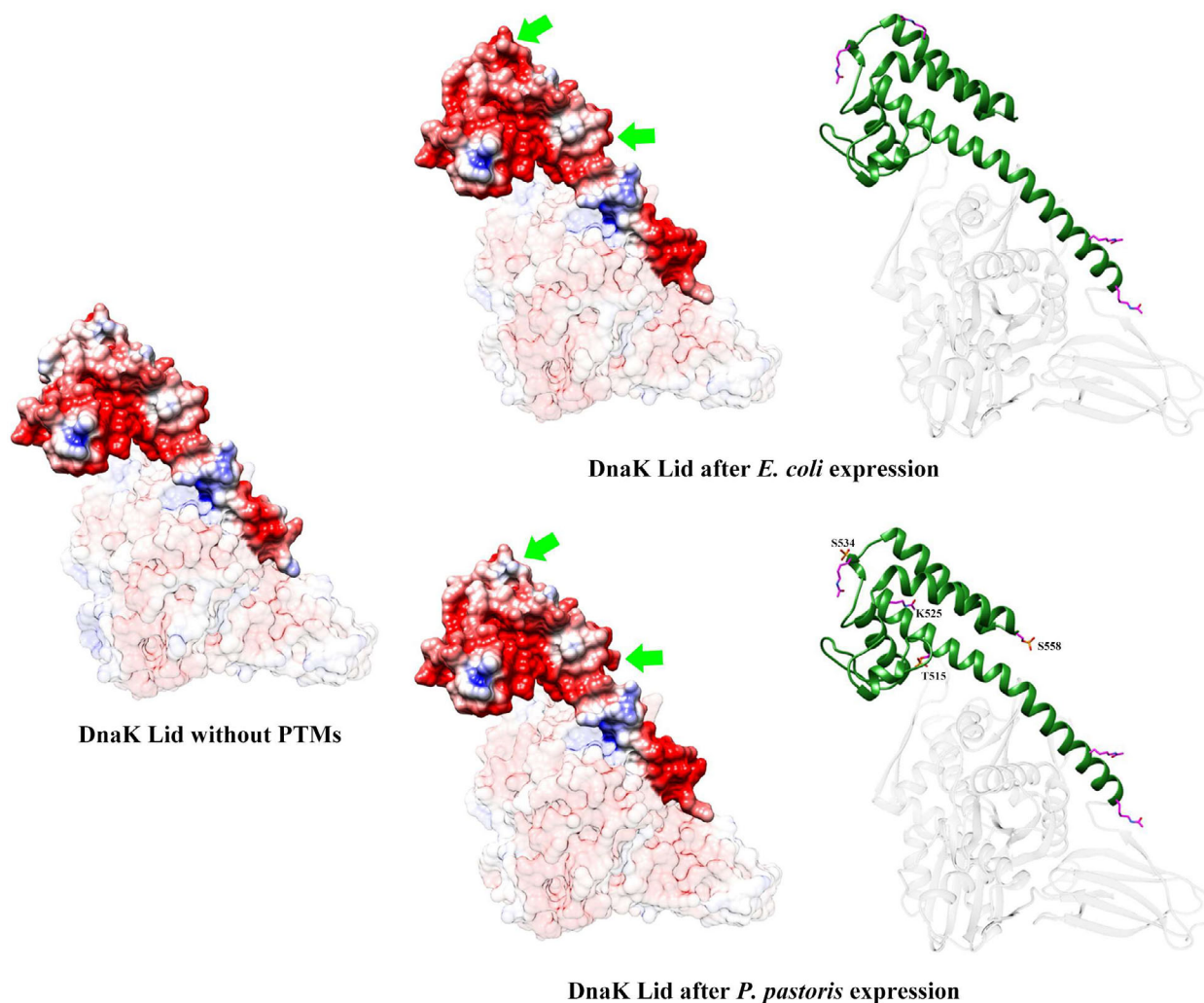


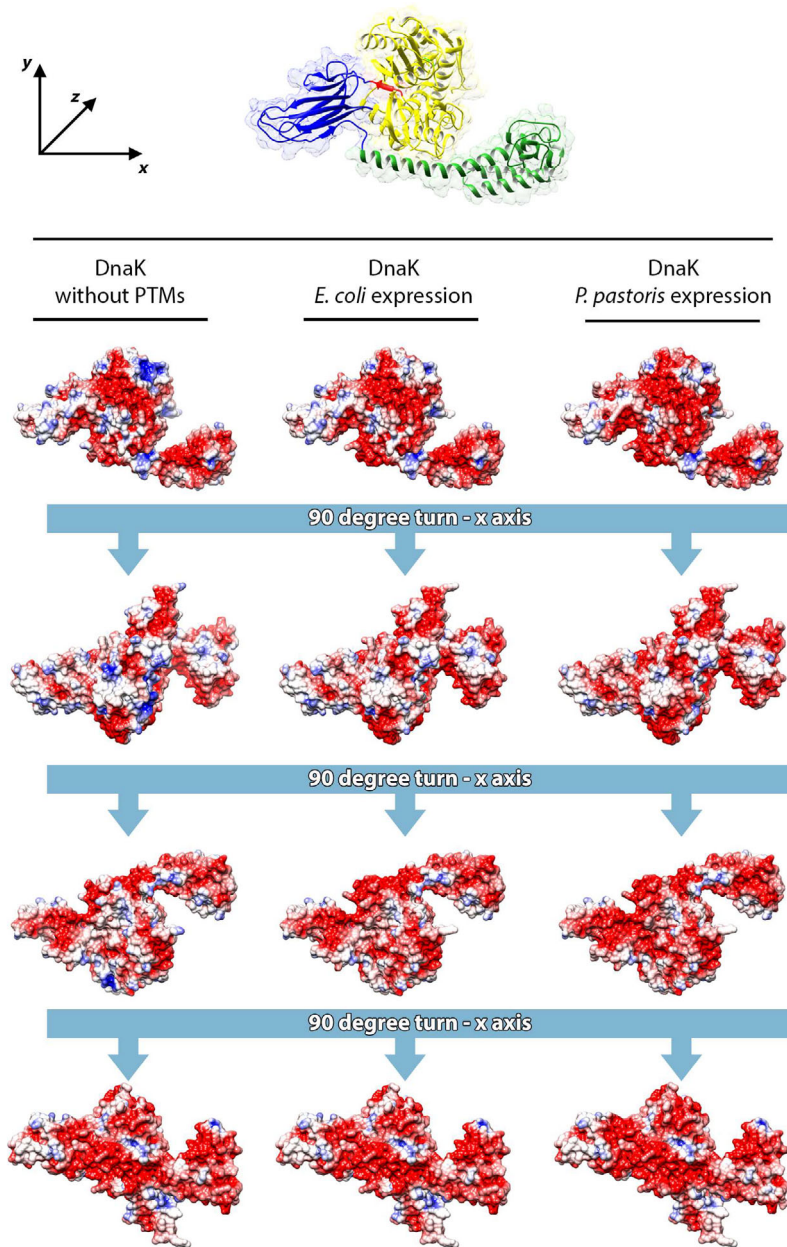
Fig. 4. Surface and ribbon representation of the DnaK model, with emphasis on the Lid domain. The electrostatic potential was computed on the surface and the color range (-3 kT to $+3$ kT, where k represents the Boltzmann constant and T represents the temperature) indicates the positive (*blue*), neutral (*white*), and negative (*red*) charges. The arrows highlight the charges and topographical differences between proteins expressed in each system. The figures were built using the software UCSF Chimera.

studies from different research groups, in spite of the same amino acid sequence.

The negative charges added to the NDB in *P. pastoris* (K55 and K240)—but not in *E. coli*—could have a direct impact on ATP hydrolysis as well as ADP-ATP exchange due to the proximity to the ADP-ATP binding site. In respect to SBD, it is known that this region favors the binding of hydrophobic, positive residues, and this is directly influenced by the electrostatic potential. DnaK expressed in *P. pastoris* had a more negative aspect in the SBD, especially influenced by the presence of an acetyl group in the lysine 378 (Fig. 5B). This points to the fact that the impact on substrate binding will be affected differently if we take into

account the presence of the PTMs. Also, the fact that most of the modified residues are not buried, but rather exposed in the surface, could have implications in protein–protein interactions either in the intracellular environment as well as in the extracellular milieu. This was already discussed by Morgner *et al.* [31] when they observed that Hsp70 expressed in different cells (*Sf9* and *E. coli*), despite the same amino acid sequence, had a different propensity to form oligomerization states, which was attributed to the presence of PTMs. Important to note that this oligomerization was formed through the lid domain, and as we described here presented a different pattern of PTMs, especially related to phosphorylation sites, depending on the expression system.

A



B

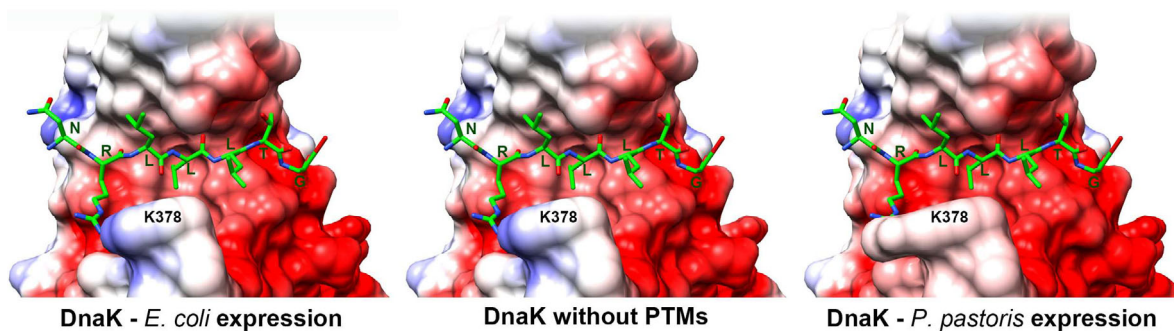


Fig. 5. Impact of the PTMs detected in DnaK expressed in different systems. (A) At the top, the DnaK model is represented. Below, the electrostatic potential surface of each protein is represented. The proteins were rotated 90° around the x-axis (according to coordinates upper left). The color range (−3 kT to +3 kT, where k represents the Boltzmann constant and T represents the temperature) indicates the positive (blue), neutral (white), and negative (red) charges. (B) Overview of SBD region and NRLLLTG (green) peptide. The binding cleft is represented as a surface colored according to electrostatic potential. Color range indicates the positive (blue), neutral (white), and negative (red) charges (−3 kT to +3 kT, where k represents the Boltzmann constant and T represents the temperature). The surface related to Lysine 378 (K378) was labeled. The figures were build using the software UCSF Chimera.

It is still unclear if, or to what extent, the extracellular properties of Hsp70 are connected to their intracellular chaperone and ATPase functions. The exact mechanisms that mediate immunomodulatory roles for Hsp70 are far from elucidated. It is unknown if it exists only as a monomer or also as an oligomer in a soluble state in plasma or extracellular spaces. Many studies reported it to be present in exosomes [32–35]. Others report Hsp70 being embedded in the plasma membrane of tumor cells [36,37]. The interactions of extracellular Hsp70s with membranes have been described as occurring via different receptors, including CD94 [38], CD40 [39], CCR5 [40], and LOX-1 [41]. The binding of ligands to scavenger receptors, for example, to LOX-1, is critically dependent on negative charges. It seems to be the key unifying property of the disparate SR ligands [42,43]. These data are in accordance with our results in which the treatment of the DnaK expressed in *P. pastoris* with an alkaline phosphatase would increase the charge of protein (Fig. 5A), thus decreasing its immunomodulatory effects over DCs (Fig. 6D,E).

Alternatively, it has been shown that both Hsp70 and DnaK can associate with lipids [44] and suggested Hsp70s would not need to engage a protein receptor to cross lipid bilayers. Arispe *et al.* (2016) compared the interactions of DnaK and Hsp70 with synthetic liposomes. They observed that mammalian Hsp70 favored association with negatively charged phospholipids, such as phosphatidylserine, whereas DnaK interacted with all lipids tested regardless of the charge. In that study, both proteins were prepared recombinantly in *E. coli*, which might have resulted in fewer negative charges as a result of post-translational modifications, and could at least in part explain their results.

Phosphatase treatment of the DnaK indicated that the phosphorylations added in the *P. pastoris* system, especially to the NBD, interfered with ATPase activity in the absence of DnaJ. One possible explanation is that the negative charges due to phosphorylation of the residues negatively affect the interaction with ATP, which is negatively charged at pH 7. DnaJ promoted ATPase activity as expected; DnaK alone has a much more modest ATPase activity compared to what is observed in the presence of DnaJ [45]. However, the

more pronounced stimulation of DnaK produced in *P. pastoris* by DnaJ does not depend on phosphorylation. It is possible that PTMs added in the *Pichia* system promote interaction of DnaK with DnaJ; alternatively, PTMs added during production in *E. coli* might inhibit DnaJ interaction.

Altogether, we believe our results can aid in the interpretation of some of the results from previous studies on extracellular properties of Hsp70, and help set some guidelines that might unify future endeavors in this field. Moreover, these results provide critical evidence on the importance of PTMs and the choice of the expression system for all studies that analyze recombinant protein interactions with cells and tissues.

Materials and methods

Protein expression and purification

Recombinant DnaK from *M. tuberculosis* (Gene ID: 885946) was expressed and purified in *P. pastoris* system by the company ProteinOne (Rockville, MD, USA). Briefly, the gene was synthesized by DNA 2.0, inserted into pJ912 vector, and transformed into *Pichia* competent cells for expression. After screening with methanol induction, high expression colonies were selected and scaled up to a 6-liter yeast expression system. Protein was purified with a Pharmacia FPLC system (GE Lifesciences, Marlborough, MA, USA) with all chromatography runs performed under clean 4 °C conditions. After purification, SDS/PAGE analysis was performed with NuPAGE 5–12% gel (Invitrogen, Carlsbad, CA, USA). Alternatively, *M. tuberculosis* DnaK gene was inserted into the pET23(a)+ plasmid, and the protein was expressed and purified from an *E. coli* system, as described in [30,46]. All proteins were quantitated with the Pierce BCA Protein assay kit (Thermo Scientific, Waltham, MA, USA).

Trypsin digestion

Gel sections 150kDa to 38kDa were excised from a 12% 1D SDS/PAGE (Invitrogen), chopped into ~1-mm pieces, washed in dH₂O, and destained using 100 mM ammonium bicarbonate (NH₄HCO₃) pH 7.5 in 50% acetonitrile. A reduction step was performed by addition of 100 μL 50 mM NH₄HCO₃ pH 7.5 and 10 μL of 200 mM tris(2-

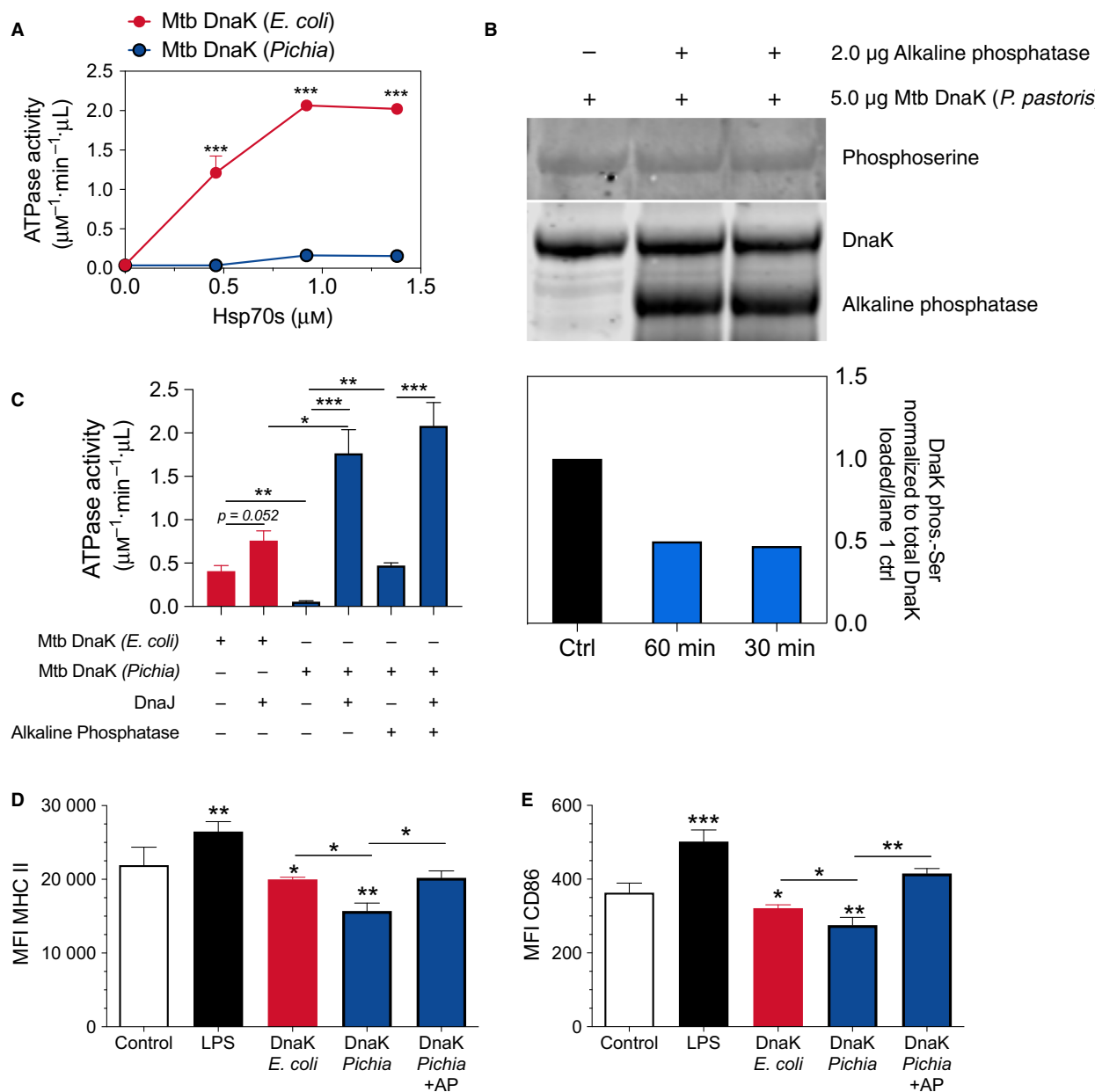


Fig. 6. Expression system-specific changes in DnaK activity. (A) ATPase activity of *M. tuberculosis* DnaK produced in *E. coli* or *P. pastoris*. Each symbol represents mean \pm SD of triplicates. Statistic by two-way ANOVA. (B) Western blot of recombinant DnaK produced in *P. pastoris* treated with or without alkaline phosphatase for 30 or 60 min at 30 °C in alkaline phosphatase buffer. Densitometry analysis represents phosphoserine signal normalized to the total DnaK loaded to each lane (lower panel, total protein stain) and as a ratio of the DnaK signal in lane 1. We observed a reduction of about 54% in phosphoserine signal. (C) ATPase activity of 0.5 μM of *M. tuberculosis* (Mtb) DnaK produced in *E. coli* or *P. pastoris* treated or not with alkaline phosphatase (AP). Mtb DnaKs were also incubated with 0.25 μM of DnaJ. Each bar represents mean \pm SD of triplicates. Statistic by one-way ANOVA with Tukey post-test. (A and C) ATPases were obtained subtracting the background blank for each protein preparation. Murine dendritic cells (DCs) were isolated from secondary lymph organs by magnetic separation. Cells were incubated with LPS (250 $\text{ng}\cdot\text{mL}^{-1}$ —positive control), DnaK produced in *E. coli* or *P. pastoris*, and the expression of (D) MHC II and (E) CD86 was analyzed by flow cytometry. Alternatively, DCs were incubated with DnaK produced *P. pastoris* treated with alkaline phosphatase (AP). All DnaK treatments were 20 $\mu\text{g}\cdot\text{mL}^{-1}$. Statistic by one-way ANOVA with Tukey post-test. Bars represent the mean \pm SD of triplicates of pooled cells from three mice per experiment. All experiments were repeated at three times.

carboxyethyl) phosphine HCl at 37°C for 30 min. The proteins were alkylated by the addition of 100 µL of 50 mM iodoacetamide prepared fresh in 50 mM NH₄HCO₃ pH 7.5 buffer, and allowed to react in the dark at 20 °C for 30 min. Gel sections were washed in water, then acetonitrile, and vacuum-dried. Trypsin digestion was carried out overnight at 37°C with 1 : 50–1 : 100 enzyme–protein ratio of sequencing grade-modified trypsin (Promega, Madison, WI, USA) in 50 mM NH₄HCO₃ pH 7.5, and 20 mM calcium chloride (CaCl₂). Peptides were extracted sequentially with 5% formic acid, then with 75% acetonitrile (ACN) in 5% formic acid, combined, and vacuum-dried.

HPLC for mass spectrometry

All samples were re-suspended in Burdick & Jackson HPLC-grade water containing 0.2% formic acid (Honeywell Fluka, Charlotte, NC, USA), 0.1% TFA (Pierce™, Thermo Scientific), and 0.002% Zwittergent 3–16 (Calbiochem, San Diego, CA, USA), a sulfobetaine detergent that contributes the following distinct peaks at the end of chromatograms: MH + at 392, and in-source dimer [2 M + H+] at 783, and some minor impurities of Zwittergent 3–12 seen as MH + at 336. The peptide samples were loaded to a 0.25 µL C8 OptiPak trapping cartridge custom-packed with Michrom Magic (Optimize Technologies, Oregon City, OR, USA) C8, washed, then switched in-line with a 20 cm by 75 µm C18 packed spray tip nanocolumn packed with Michrom Magic C18AQ, for a 2-step gradient. Mobile phase A was water/acetonitrile/formic acid (98/2/0.2), and mobile phase B was acetonitrile/isopropanol/water/formic acid (80/10/10/0.2). Using a flow rate of 350 nL·min⁻¹, a 90 min, 2-step LC gradient was run from 5% B to 50% B in 60 min, followed by 50–95% B over the next 10 min, hold 10 min at 95% B, back to starting conditions and re-equilibrated.

LC–MS/MS analysis

The samples were analyzed via electrospray tandem mass spectrometry (LC–MS/MS) on a Thermo Q-Exactive Orbitrap mass spectrometer, using a 70 000 RP survey scan in profile mode, m/z 360–2000 Da, with lock masses, followed by 20 MS/MS HCD fragmentation scans at 17 500 resolution on doubly and triply charged precursors. Single charged ions were excluded, and ions selected for MS/MS were placed on an exclusion list for 60s, and dynamic exclusion turned off. An inclusion list of expected bait protein proteolytic peptide ions predicted to have PTMs (phosphorylation, ubiquitination, or acetylation) was used allowing for other ions.

Database searching

Tandem mass spectra were extracted by Proteo wizard version 3.0.9.134. Charge state deconvolution and deisotoping

were performed. All MS/MS samples were analyzed using Mascot (Matrix Science, London, UK; version 2.3.02) and X! Tandem [The GPM, thegpm.org; version CYCLONE (2010.12.01.1)]. Mascot and X! Tandem were set up to search Human, Mus, or MTB databases {150821_SPROT_Human_Iso_AUP000005640 database (unknown version, 91618 entries), 151218_SPROT_MTB_UP000001584 database (unknown version, 3993 entries), or 150612_Mus_uniprot_proteome_AUP000000589 database (unknown version, 45182 entries)}. Mascot and X! Tandem were searched with a fragment ion mass tolerance of 0.40 Da and a parent ion tolerance of 10.0 PPM. Carbamidomethyl of cysteine was specified in Mascot and X! Tandem as a fixed modification. Deamidation of asparagine and glutamine; oxidation of methionine; formyl of the N terminus; acetyl of lysine; phospho of serine, threonine, and tyrosine; and Gly-Gly of lysine were specified in Mascot as variable modifications. Glu->pyro-Glu of the N terminus; ammonia-loss of the N terminus; gln->pyro-Glu of the N terminus; deamidation of asparagine and glutamine; oxidation of methionine; formyl of the N terminus; acetyl of lysine; phospho of serine, threonine, and tyrosine; and Gly-Gly of lysine were specified in X! Tandem as variable modifications.

Criteria for protein identification

Scaffold (version Scaffold_4.8.4, PROTEOME Software Inc., Portland, OR, USA) was used to validate MS/MS-based peptide and protein identifications. Peptide identifications were accepted if they could be established at greater than 27.0% probability to achieve an FDR less than 1.0%. Peptide Probabilities from Mascot (Ion Score Only) were assigned by the Scaffold Local FDR algorithm. Peptide Probabilities from X! Tandem were assigned by the Peptide Prophet algorithm [47] with Scaffold delta-mass correction. Protein identifications were accepted if they could be established at greater than 92.0% probability to achieve an FDR less than 1.0% and contained at least 2 identified peptides. Protein probabilities were assigned by the Protein Prophet algorithm [48]. Proteins that contained similar peptides and could not be differentiated based on MS/MS analysis alone were grouped to satisfy the principles of parsimony. Proteins sharing significant peptide evidence were grouped into clusters.

Alkaline phosphatase treatment

About 2.0 µg alkaline phosphatase (Sino biological, cat. no. 10440-H08H) was incubated with 5.0 µg DnaK *P. pastoris* for 30 or 60 min as indicated at 30 °C in a 35-µL reaction consisting of 22 µL alkaline phosphatase buffer (100 mM NaCl, 100 mM Tris/Cl, 50 mM MgCl₂), 8 µL of alkaline phosphatase enzyme, and 5 µL of DnaK. This preparation was up-scaled to prepare DnaK for

experiments involving the treatment of dendritic cells and ATPase assays. To quantify the level of dephosphorylation, 35- μ L preparations were mixed with 8.75 μ L 4x LDS sample buffer (GenScript, Piscataway, NJ, USA, cat. no. M00676)/ β -mercaptoethanol and heated at 70°C for 10 mins. Samples were then resolved by size by SDS/PAGE for 40 mins at 200V on a 4–12% Bis-Tris gel (GenScript, cat. no. M00652) using MOPS running buffer. Western transfer to Immobilon-FL membranes (Millipore, cat. no. IPFL00010) was performed at 100 V for 60 mins using the wet-transfer method, transfer buffer (Boston Bioproducts, cat. no. BP-190, 15% methanol). The membrane was then stained using REVERT Total Protein stain (LICOR, cat. no. 926-11011), and washed in REVERT wash solution (926-11012) and imaged on an Odyssey CLx. The membrane was then blocked with Odyssey TBS blocking buffer (LICOR, cat. no. 927-50000) for 1 h at RT and then probed with anti-phosphoserine antibody (ab9332) at 1 : 100 overnight at 4°C in TBS blocking buffer/0.2% Tween-20. Unbound primary antibody was removed by washing in TBST, and anti-rabbit IRDye800CW (cat. no. 925-32211) secondary antibody was added at 1 : 15 000 dilution in TBS blocking buffer/ 0.2% Tween-20/ 0.01% SDS and incubated at RT with agitation for 30 mins. The membrane was then again imaged on an Odyssey CLx after removal of unbound secondary antibody by washing in 4x 5mins in TBST and 1x 5mins in TBS at RT.

ATPase activity assay

Steady-state ATPase activity was measured using the ATPase/GTPase Activity Assay kit (Sigma-Aldrich), according to the manufacturer's protocol. Assays were performed at room temperature for 2h using 4 mM of ATP (Sigma). DnaK concentrations were 0.5, 1, or 1.5 μ M for both proteins. In some experiments, 0.5 μ M of native or AP-treated DnaK expressed in *P. pastoris* or 0.5 μ M of DnaK expressed in *E. coli*. DnaKs were also incubated with 0.25 μ M of *E. coli* DnaJ (from RayBiotech). Reactions were monitored by measuring the absorbance decay three times at 630 nm in a Versa Max plate reader (Molecular Devices). ATPase activity was determined against a standard phosphate curve.

Animal and study approval

C57Bl/6 mice were from The Jackson Laboratory. Animals in the experiments were females between six to 10 weeks old. All animals were housed in accordance with the Institutional Animal Care and Use Committee (IACUC) and National Institutes of Health (NIH) Animal Care guidelines. Experiments were approved by the BIDMC Animal Care Use Committee under IACUCC0792012.

In vitro modulation of murine dendritic cells

CD11c⁺ cells were isolated from LNs and spleens of B6 WT mice. LNs and spleens were disrupted in a cell strainer and treated with Collagenase D (Roche) for 30 min at 37 °C. Cells were labeled with anti-CD11c (N418) magnetic beads (Miltenyi). CD11c⁺ cells were subsequently purified by positive selection using MACS separation columns (Miltenyi). The purity of selected cells (CD11c^{high}MHCII^{high} cells) was controlled by flow cytometry and cells only used when purity was \geq 85% (not shown). Cells were cultured in 24-well plates in serum-free medium (AIM-V, Gibco). DCs were incubated in media (control), media containing 20 μ g-mL⁻¹ of *M. tuberculosis* DnaK produced in *E. coli* or *P. pastoris* or 250 ng-mL⁻¹ of *E. coli* LPS (Sigma) for 24h. Cells were analyzed by flow cytometry.

Flow cytometry

The following antibodies were used: I-Ab (AF6-120.1), CD11c (HL3), CD86 (GL1), from BD Biosciences (Franklin Lakes, NJ, USA); CD19 (6D5), CD3 (145-2C11), and CD11c (N418) from Biolegend. Cells were Fc blocked for 20 min on ice, and then, surface markers were stained by incubation for 30 min with antibodies in 2% FBS in PBS 1x on ice. Cells were analyzed using FACSCantoII (BD Biosciences) and BD FACSDIVA software (BD Biosciences). Dead cells were excluded by staining with Fixable Viability Dye eFluor 780 (eBioscience). Data were analyzed using FLOWJO software (version X, Tree Star).

DnaK modeling/ab initio and validation

The use of homology modeling process requires a first step of search for templates. The search was performed using BLAST (*PDB database*) and HHPRED server using as input the FASTA sequence of DnaK. The best templates were chosen based on coverage, similarity, presence of gaps, and identity of residues. Modeling was performed using MODELLER v9.10 software (homology modeling) and ROSETTA server (*ab initio* and/or homology modeling). With Modeller, the variable target function method (VTFM) was used to optimize the models, which were assessed through DOPE score. A total of 100 models were generated and ranked. In the end, the 10 best models were chosen to pass through a set of validation servers, which included Verify3D, QMEAN, ProQ, ModEval, and Rampage. The model with the best mean score among the validation servers was chosen. ROSETTA was used to model a C-terminal region of the protein that lacks homology with any available three-dimensional structure. The Ginzu protocol from ROSETTA was used to build the best model of this region, which was united with the rest of the protein with Modeller. In this stage, a set of 100 models is

generated, which were also assessed with the same validation servers to choose the most accurate.

Electrostatic potential analysis

DelPhi program was used to assess the electrostatic potential of each molecule. The grid spacing (grids/angstrom) was set to 1.0. The perfil (percentage of the object longest linear dimension to the lattice linear dimension) was set to 80 and the grid size to 251. The internal and external dielectric constants were maintained 1.0 (molecule with no polarizability) and 80.0 (molecule in water), respectively. A probe radius was configured to 1.4 angstroms and the concentration of the first kind of salt to 0.2 moles·L⁻¹. The electrostatic potential was represented through color patterns (blue, white, and red) in terms of kT , where k represents the Boltzmann constant and T represents the temperature. The software UCSF Chimera version 12 was used to compute and visualize the electrostatic potential of the protein surface.

In silico insertion of post-translational modifications

Individual PTMs were inserted in each molecule using PyTMs, a PyMOL plug-in for modeling of common PTMs. Here, we work specifically with acetylation and phosphorylation. The acetylation was targeted against the side chain atoms of lysine residues, while the phosphorylation was inserted in serine, threonine, or tyrosine side chain's residues.

Acknowledgements

This study was financed by Coordenação de Aperfeiçoamento de Pessoal de Nível Superior (CAPES)—Finance Code 001 to MMR; Conselho Nacional de Desenvolvimento Científico e Tecnológico (CNPq)—grant number 422164/2018-6 and 306572/2018-9 to CB; NIH grant number RO1CA176326 to SKC.; and NCI R15 CA208773 to AWT.

Conflict of interest

The authors declare no conflict of interest.

Author contributions

MMR, TJB, AWT, and CB conceived and designed the idea of the work. MMR, TJB, and CB wrote the main text of the paper aided by SKC and AWT. MMR performed all bioinformatics experiments and analyses. TJB, BJL, and AM performed experiments involving ATPase activity. TJB performed the

experiments involving DC modulation. BJL performed DnaK treatment with AP and blots. N, DW, and AWT expressed, collected, purified, performed the mass spectrometry, and analyzed the data. MMR, TJB, BJL, AM, SKC, AWT, and CB revised the final version of the paper before submission. All authors participated in the analysis and discussion of the data and approved the final version of the manuscript.

References

- Craig EA & Marszalek J (2017) How do J-proteins get Hsp70 to do so many different things? *Trends Biochem Sci* **42**, 355–368.
- Kim YE, Hipp MS, Bracher A, Hayer-Hartl M & Hartl FU (2013) Molecular chaperone functions in protein folding and proteostasis. *Annu Rev Biochem* **82**, 323–55.
- Nillegoda NB, Wentink AS & Bukau B (2018) Protein disaggregation in multicellular organisms. *Trends Biochem Sci* **43**, 285–300.
- Rosenzweig R, Nillegoda NB, Mayer MP & Bukau B (2019) The Hsp70 chaperone network. *Nat Rev Mol Cell Biol* **20**, 665–680.
- Mayer MP (2018) Intra-molecular pathways of allosteric control in Hsp70s. *Philos Trans R Soc Lond B Biol Sci* **373**, pii: 20170183.
- Mayer MP & Bukau B (2005) Hsp70 chaperones: cellular functions and molecular mechanism. *Cell Mol Life Sci* **62**, 670–684.
- Xu L, Nitika Hasin N, Cuskelly DD, Wolfgeher D, Doyle S, Moynagh P, Perrett S, Jones GW & Truman AW (2019) Rapid deacetylation of yeast Hsp70 mediates the cellular response to heat stress. *Sci Rep* **9**, 16260.
- Zemanovic S, Ivanov MV, Ivanova LV, Bhatnagar A, Michalkiewicz T, Teng R-J, Kumar S, Rathore R, Pritchard KA, Konduri GG *et al.* (2018) Dynamic phosphorylation of the C terminus of Hsp70 regulates the mitochondrial import of SOD2 and redox balance. *Cell Rep* **25**, 2605–2616.e7.
- Lim S, Kim DG & Kim S (2019) ERK-dependent phosphorylation of the linker and substrate-binding domain of HSP70 increases folding activity and cell proliferation. *Exp Mol Med* **51**, 112.
- Cloutier P & Coulombe B (2013) Regulation of molecular chaperones through post-translational modifications: decrypting the chaperone code. *Biochim Biophys Acta* **1829**, 443–454.
- Nitika & TrumanAW (2017) Cracking the Chaperone code: Cellular roles for Hsp70 phosphorylation. *Trends Biochem Sci* **42**, 932–935.
- Velazquez JM, DiDomenico BJ & Lindquist S (1980) Intracellular localization of heat shock proteins in *Drosophila*. *Cell* **20**, 679–689.

- 13 Lindquist S (1986) The heat-shock response. *Annu Rev Biochem* **55**, 1151–1191.
- 14 Lindquist S & Craig EA (1988) The heat-shock proteins. *Annu Rev Genet* **22**, 631–677.
- 15 Hightower LE & Guidon PT (1989) Selective release from cultured mammalian cells of heat-shock (stress) proteins that resemble glia-axon transfer proteins. *J Cell Physiol* **138**, 257–266.
- 16 Hunter-Lavin C, Davies EL, Bacelar MMFVG, Marshall MJ, Andrew SM & Williams JHH (2004) Hsp70 release from peripheral blood mononuclear cells. *Biochem Biophys Res Commun* **324**, 511–517.
- 17 Zhan R, Leng X, Liu X, Wang X, Gong J, Yan L, Wang L, Wang Y, Wang X & Qian L-J (2009) Heat shock protein 70 is secreted from endothelial cells by a non-classical pathway involving exosomes. *Biochem Biophys Res Commun* **387**, 229–233.
- 18 Mambula SS & Calderwood SK (2006) Heat shock protein 70 is secreted from tumor cells by a nonclassical pathway involving lysosomal endosomes. *J Immunol* **177**, 7849–7857.
- 19 Asea A, Kraeft SK, Kurt-Jones EA, Stevenson MA, Chen LB, Finberg RW, Koo GC & Calderwood SK (2000) HSP70 stimulates cytokine production through a CD14-dependant pathway, demonstrating its dual role as a chaperone and cytokine. *Nat Med* **6**, 435–442.
- 20 Gao B & Tsan M-F (2003) Endotoxin contamination in recombinant human heat shock protein 70 (Hsp70) preparation is responsible for the induction of tumor necrosis factor alpha release by murine macrophages. *J Biol Chem* **278**, 174–179.
- 21 Bendz H, Marincek B-C, Momburg F, Ellwart JW, Issels RD, Nelson PJ & Noessner E (2008) Calcium signaling in dendritic cells by human or mycobacterial Hsp70 is caused by contamination and is not required for Hsp70-mediated enhancement of cross-presentation. *J Biol Chem* **283**, 26477–26483.
- 22 Calderwood SK, Murshid A & Gong J (2012) Heat shock proteins: conditional mediators of inflammation in tumor immunity. *Front Immunol* **3**, 75.
- 23 Borges TJ, Lang BJ & Lopes RL & Bonorino C (2016) Modulation of alloimmunity by heat shock proteins. *Front Immunol* **7**, 303.
- 24 Porro D, Gasser B, Fossati T, Maurer M, Branduardi P, Sauer M & Mattanovich D (2011) Production of recombinant proteins and metabolites in yeasts: when are these systems better than bacterial production systems? *Appl Microbiol Biotechnol* **89**, 939–948.
- 25 Dworkin J (2015) Ser/Thr phosphorylation as a regulatory mechanism in bacteria. *Curr Opin Microbiol* **24**, 47–52.
- 26 Brown CW, Sridhara V, Boutz DR, Person MD, Marcotte EM, Barrick JE & Wilke CO (2017) Large-scale analysis of post-translational modifications in *E. coli* under glucose-limiting conditions. *BMC Genom* **18**, 301.
- 27 Borges TJ, Wieten L, van Herwijnen MJC, Broere F, van der Zee R, Bonorino C & van Eden W (2012) The anti-inflammatory mechanisms of Hsp70. *Front Immunol* **3**, 95.
- 28 Khoury GA, Baliban RC & Floudas CA (2011) Proteome-wide post-translational modification statistics: frequency analysis and curation of the swiss-prot database. *Sci Rep* **1**, pii: srep00090.
- 29 Motta A, Schmitz C, Rodrigues L, Ribeiro F, Teixeira C, Detanico T, Bonan C, Zwickey H & Bonorino C (2007) Mycobacterium tuberculosis heat-shock protein 70 impairs maturation of dendritic cells from bone marrow precursors, induces interleukin-10 production and inhibits T-cell proliferation in vitro. *Immunology* **121**, 462–472.
- 30 Borges TJ, Murakami N, Machado FD, Murshid A, Lang BJ, Lopes RL, Bellan LM, Uehara M, Antunes KH, Pérez-Saéz MJ *et al.* (2018) March1-dependent modulation of donor MHC II on CD103+ dendritic cells mitigates alloimmunity. *Nat Commun* **9**, 3482.
- 31 Morgner N, Schmidt C, Beilstein-Edmands V, Ebong I-O, Patel NA, Clerico EM, Kirschke E, Daturpalli S, Jackson SE, Agard D *et al.* (2015) Hsp70 forms antiparallel dimers stabilized by post-translational modifications to position clients for transfer to Hsp90. *Cell Rep* **11**, 759–769.
- 32 Lancaster GI & Febbraio MA (2005) Exosome-dependent trafficking of HSP70: a novel secretory pathway for cellular stress proteins. *J Biol Chem* **280**, 23349–23355.
- 33 Simpson RJ, Jensen SS & Lim JWE (2008) Proteomic profiling of exosomes: Current perspectives. *Proteomics* **8**, 4083–4099.
- 34 Théry C, Zitvogel L & Amigorena S (2002) Exosomes: composition, biogenesis and function. *Nat Rev Immunol* **2**, 569–579.
- 35 Chen T, Zhang G, Kong L, Xu S, Wang Y & Dong M (2019) Leukemia-derived exosomes induced IL-8 production in bone marrow stromal cells to protect the leukemia cells against chemotherapy. *Life Sci* **221**, 187–195.
- 36 Stangl S, Gehrman M, Riegger J, Kuhs K, Riederer I, Sievert W, Hube K, Mocikat R, Dressel R, Kremmer E *et al.* (2011) Targeting membrane heat-shock protein 70 (Hsp70) on tumors by cmHsp70.1 antibody. *Proc Natl Acad Sci USA* **108**, 733–738.
- 37 Multhoff G (2007) Heat shock protein 70 (Hsp70): membrane location, export and immunological relevance. *Methods* **43**, 229–237.
- 38 Gross C, Hansch D, Gastpar R & Multhoff G (2003) Interaction of heat shock protein 70 peptide with NK cells involves the NK receptor CD94. *Biol Chem* **384**, 267–279.

- 39 Zininga T & Ramatsui L & Shonhai A (2018) Heat shock proteins as immunomodulators. *Molecules* **23**, 2846.
- 40 Whittall T, Wang Y, Younson J, Kelly C, Bergmeier L, Peters B, Singh M & Lehner T (2006) Interaction between the CCR5 chemokine receptors and microbial HSP70. *Eur J Immunol* **36**, 2304–2314.
- 41 Delneste Y, Magistrelli G, Gauchat J, Haeuw J, Aubry J, Nakamura K, Kawakami-Honda N, Goetsch L, Sawamura T, Bonnefoy J *et al.* (2002) Involvement of LOX-1 in dendritic cell-mediated antigen cross-presentation. *Immunity* **17**, 353–362.
- 42 Shi X, Niimi S, Ohtani T & Machida S (2001) Characterization of residues and sequences of the carbohydrate recognition domain required for cell surface localization and ligand binding of human lectin-like oxidized LDL receptor. *J Cell Sci* **114**, 1273–1282.
- 43 Park H, Adsit FG & Boyington JC (2005) The 1.4 angstrom crystal structure of the human oxidized low density lipoprotein receptor lox-1. *J Biol Chem* **280**, 13593–13599.
- 44 Lopez V, Cauvi DM, Arispe N & De Maio A (2016) Bacterial Hsp70 (DnaK) and mammalian Hsp70 interact differently with lipid membranes. *Cell Stress Chaperones* **21**, 609–616.
- 45 Russell R, Wali Karzai A, Mehl AF & McMacken R (1999) DnaJ dramatically stimulates ATP hydrolysis by DnaK: insight into targeting of Hsp70 proteins to polypeptide substrates. *Biochemistry* **38**, 4165–4176.
- 46 Lopes RL, Borges TJ, Zanin RF & Bonorino C (2016) IL-10 is required for polarization of macrophages to M2-like phenotype by mycobacterial DnaK (heat shock protein 70). *Cytokine* **85**, 123–129.
- 47 Keller A, Nesvizhskii AI, Kolker E & Aebersold R (2002) Empirical statistical model to estimate the accuracy of peptide identifications made by MS/MS and database search. *Anal Chem* **74**, 5383–5392.
- 48 Nesvizhskii AI, Keller A, Kolker E & Aebersold R (2003) A statistical model for identifying proteins by tandem mass spectrometry. *Anal Chem* **75**, 4646–4658.

Supporting information

Additional supporting information may be found online in the Supporting Information section at the end of the article.

Movie S1. Visualization of all proteins with the electrostatic potential calculated.

Table S1. PTM sites for DnaK expressed in *E. coli*.

Table S2. PTM sites for DnaK expressed in *P. pastoris*.